Global sensitivity analysis of dike stability under maximum static groundwater heads

Teun van Woerkom [1], Rens van Beek [1], Hans Middelkoop [1], Marc F.P. Bierkens [1,2]

[1]University of Utrecht, Faculty of Geosciences, Department of Physical Geography, P.O. 80.115, Utrecht, the Netherlands
[2]Unit Soil and Groundwater Systems, Deltares, P.O. 85467, Utrecht, the Netherlands

Key Points:

- Worst case stability of dikes is mostly influenced by dike geometry and material
- Dike and shallow subsurface material feedback leads to unexpected results
- A Monte-Carlo analysis using a hydro-stability model can target stability assessment investigations

Corresponding author: Teun van Woerkom, `t.a.a.vanwoerkom@uu.nl`

Abstract

With a large network of dikes that in the future will protect up to 15% of the world's population from flooding, more extreme river discharges that result from climate change will dramatically increase the flood risk of these protected societies. Precise calculations of dike stability under adverse loading conditions will become increasingly important, though the hydrological impacts on dike stability, particularly the effects of groundwater flow, are often oversimplified in stability calculations. To include these effects, we use a coupled hydro-stability model to indicate relations between the geometry, subsurface materials, groundwater hydrology and stability of a dike regarding soil slip and basal sliding mechanisms. Sensitivity analyses are performed with this model using a large number of parameter combinations, while assessing both the individual sensitivity as combined effects. The analyses show that the material type of the dike and its slope are the more important parameters influencing the stability, followed by the shallow subsurface type and dike crest elevation. The material of the dike and shallow subsurface is additionally important, as a change towards sandier material can either result in either an increase or a decrease of the stability. A database created by an extensive Monte Carlo analysis provides further evidence for these relations and is used to estimate failure probabilities for dike stretches that have not been assessed in detail. Despite the use of a simplified model, not including small-scale heterogeneity, remaining soil strength and transient groundwater flow, the application of the method to a case study proves its applicability.

1 Introduction

The number of people in Europe that is at risk of flooding is estimated at a minimum of 50 million. Over 45 flood events occurred between 1950 and 2005 that each resulted in at least 70 fatalities and an economical damage of 0.005% of the European GDP (Tourment, 2018). With global population growth, it is expected that in 2050 15% of the worlds population will be living in areas that are flood-prone, increasing the probability of high-impact floods. Many flood prone rivers therefore have an extensive dike network, which along Europe's major rivers stretches for approximately 60,000 km (ICOLD, 2018). To ensure the safety of people living behind dikes, continuous maintenance and reinforcements are needed to warrant the stability of dikes and their proper functioning under high water events. Climate change, through for example earlier snow melt or an increase in extreme precipitation events in the upstream drainage area (IPCC, 2014), poses a new threat that may increase the risk of a society to flooding (Middelkoop et al., 2001). To maintain safety levels, major investments are needed for dike maintenance and reinforcement, of which the costs for the latter are in the order of 1-20 million euros per kilometer (Tourment, 2018). Improved knowledge of the processes that may occur during or following a high water event and can lead to dike failure is crucial for more cost-effective dike reinforcements, which may reduce the total expenditures on dike reinforcements substantially and can support more societally acceptable flood defense measures (Eijgenraam et al., 2014).

To reduce the hazard of dike failure under the adverse loading conditions of higher groundwater levels and river stages during and following high water events, multiple failure mechanisms have to be taken into account. In contrast to overtopping, basal sliding and soil slip are related to the occurrence of groundwater conditions in and below a dike, and do not require river stages that exceed the dike crest. Whether the groundwater conditions are critical or not, depends ultimately on the properties of the material within and below the dike and on the dike geometry. In response to elevated river stages, the changing groundwater conditions may increase the pore pressure and thus reduce the effective normal strength, while at the same time increasing the lateral load of river water pushing against the dike. As a consequence, parts of its inner or outer flank may slip or the dike as a whole may slide along its base (soil slip sensu lato). These mechanisms threaten the structural integrity of the dike and may lead to failure and the subsequent flooding of the hinterland. Furthermore, the local groundwater gradient between the elevated river stage and the lower level in the hinterland of the dike may cause the soil to burst open and pipes to form along which the increased flow rates are high enough to entrain material, thereby further weakening the base of the dike (Richards & Reddy, 2007). The analyses presented in this paper focuses on soil slip only, as this mechanism has a more direct link to dike failure.

While critical groundwater heads are a prerequisite for the onset of soil slip and are primarily driven by the occurrence and nature of high water events, their variation in space and time also depends on the subsurface characteristics, which are known to be highly heterogeneous both within and below dikes (Olthof, van Boheemen, Danner, Hooiveld, & de Vries, 2009; Stafleu & Dubelaar, 2016). This heterogeneity consists of both large scale variations related to fluvial or coastal architectural elements, and small scale heterogeneity in layer thickness and composition. In river areas where sandy channel deposits are embedded and covered by clayey overbank deposits (Berendsen, 1982), known large scale variations of importance include the confining layer length, which can increase or decrease the hydraulic gradient in the coarser sands below (Meehan & Benjasupattananan, 2012; Richards & Reddy, 2007). The properties of the aquifer material below the confining layer are also of importance, for example grain diameter and grain size distribution (Förster, van den Ham, Calle, & Kruse, 2012). These are known to have a systematic trend throughout a delta, but also vary across finer resolutions, changing hydrological permeability and possibly elevating pore pressures locally.

The subsurface conditions and geometry influence the hydrological response during high water events, resulting in the strength that may eventually be mobilized. This relation therefore provides a key control on the long-term stability of dikes and needs to be considered to obtain adequate designs that are neither over-designed, thus avoiding unnecessary costs, or undersized, leading to the even costlier risk of failure. To qualify and quantify this relation, previous studies focused on groundwater flow through and underneath dikes, often focused on heterogeneity in the dike or the effect of artificial reinforcements (Mateo-Lázaro, Sánchez-Navarro, García-Gil, Edo-Romero, & Castillo-Mateo, 2016; Peñuela, 2013). In these cases either the variation in hydraulic conditions (Stanisz, Borecka, Pilecki, & Kaczmarczyk, 2017) or the variation in subsurface material is limited (Mateo-Lázaro et al., 2016). Other research performed analyses in terms of the undrained strength, with the notion that it would constitute a worst-case assessment of the stability (Stark, Choi, & Lee, 2009). We hypothesize that ignoring the hydrological influence of the varying subsurface conditions may lead to an underestimation of the dominant failure mechanism with the aforementioned undesirable effect on dike design. Some researchers acknowledged this effect, and studied the influence of material properties (Lanzafame, Teng, & Sitar, 2017) or geometry (Vahedifard, Sehat, & Aanstoos, 2017) on the stability of embankments. Others successfully analyzed the effect of both geometry and material properties on groundwater seepage under and through the dike (Meehan & Benjasupattananan, 2012; Polanco & Rice, 2014), but did not link their results to the dike's stability.

In order to perform a full analysis of the process, both hydrological and stability information needs to be included in a large number of simulations. Therefore, to clarify the interaction between the hydrological and mechanical influence of the subsurface variability and the dike geometry, we performed a global sensitivity analysis of dike stability by coupling a high-resolution groundwater model with a limit equilibrium stability analysis. To constrain our results and to highlight first-order relationships, we evaluated the stability under the most critical loading conditions and the maximum pore water pressures for three failure mechanisms that affect the macro-stability of a dike, being soil slips on the inner or outer flank of the dike and basal sliding, as their occurrence is directly linked to the geometry of a dike and its composition. The goal of this analysis is to identify the overall stability of a dike in terms of its factor of safety (F) under varying hydrological loading, subsurface conditions and geometries, and including pore pressure calculations. The focus will be on (1) determining the most sensitive relations between model parameters and dike stability, (2) identifying combinations of model parameter values that lead to unexpected results and (3) constructing a database with safety factors and failure probabilities. The outcome of this global sensitivity analysis can be used to inform semi-qualitative assessments of dike stability as often applied in regional inventories, and the large set of possible combinations even allows for a direct comparison to actual cases.

2 Methods

To reach these goals, our analysis considered the dike safety regarding three types of macro-stability. Stability was expressed by means of the factor of safety (F) that was calculated using limit equilibrium methods. In these assessments, the pore pressure conditions were determined for the most critical condition and used in combination with drained soil strength parameters. The pore pressure conditions were obtained from steady-state hydrological simulations under the most adverse conditions using MODFLOW 6 software (Hughes, Langevin, & Banta, 2017; Langevin et al., 2018), for which the input files were automatically prepared. The following sections first explain the technical details about the hydro-stability model, the setup parameters, before explaining the workflow to analyse the results and answering the research questions.

2.1 Hydrological model input and calculations

The hydrological part consisted of a 2D MODFLOW model containing a cross-section from the river to behind the dike, which was created using 15 design parameters. The topography of the cross-section is defined by the dike height (D_h), dike crest width (D_w), dike slope (D_s) and floodplain width (F_w) (Figure 1). The river bed slope (R_s) is kept constant, and the river depth (R_d) is kept at a fixed ratio to the thickness of the subsurface (Table 1). The subsurface is sub-divided in three sections: the dike and two subsurface layers. The geometry of the upper and lower subsurface layers are defined by their thickness, U_{thck} and L_{thck} respectively. In addition, the dike, upper layer and lower layer are each associated with their own material type (D_{typ}, U_{typ}, L_{typ}). The material type represents a single lithological class, which is linked to the hydraulic conductivity (K_{sat}). The material types are centered on the values 1-5, but can take any real value in this range (Figure 2). The linked parameters are in that case interpolated linearly between the associated class midst. Human management is included in the model schematization

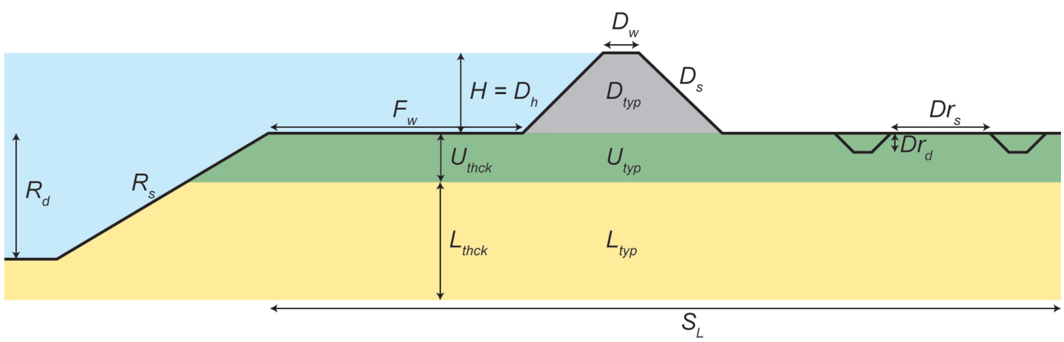

Figure 1. Schematization of all important model inputs, indicating the setup of the hydrological model. See for their meaning, values and possible ranges Tables 1 - 2.

Table 1. Name, symbol and range of the model parameters. A visualization of each of the parameters is shown in Figure 1.

Parameter	Symbol	Range	Unit
Dike height	D_h	5-10	m
Dike crest width	D_w	2-5	m
Dike slope	D_s	0.2-1	m/m
Dike type	D_{typ}	1-5	-
Upper layer thickness	U_{thck}	0.3-2	m
Upper layer type	U_{typ}	1-5	-
Lower layer thickness	L_{thck}	5-10	m
Lower layer type	L_{typ}	1-5	-
Floodplain width	F_w	0-100	m
Drainage depth	Dr_d	0.2-2	m
Drainage spacing	Dr_s	10-50	m
Surface stretch length	S_L	200	m
River bed slope	R_s	0.33	m/m
River depth	R_d	$0.9 * (U_{thck} + L_{thck})$	m
Flood height	H	D_h	m

through varying the drainage conditions behind the dike. Drainage practice is characterized by a drain spacing (Dr_s) and a drainage depth (Dr_d). Each of these parameters has a probable range in which they are sampled during their analysis (Table 1). Finally, the flood height H is assigned at the maximum dike elevation D_h, as it is assumed that under these conditions the dike reaches its most critical safety. Given a set of parameters, the MODFLOW input is automatically generated, after which a steady-state hydrological simulation is performed.

The hydrological model is setup using a cell size of 0.5 m in all directions, to assess the spatial variation at a small spatial scale while retaining the computational efficiency needed for the large number of calculations. The model is constrained by the river water level and drain depth. On the river side, the imposed river stage at the top of the dike constitutes a head-controlled boundary condition and the interaction with the groundwater is handled by the river package. Head-controlled conditions also occur on the inner side of the dike, at the ditches, which are handled by the drain package, which

Table 2. Subsurface types used in the model, related to the D_{typ}, U_{typ} and L_{typ} parameters. The subsurface type value is linked to the hydraulic conductivity (K_{sat}), porosity (P), drained cohesion (C), bulk unit weight (ρ) and effective friction angle (ϕ).

Value	Subsurface type	K_{sat} (m day^{-1})	P (-)	C (N m^{-2})	ρ (kg m^{-3})	ϕ (^{o})
1	Clay	0.0001	0.6	32000	1825	19
2	Clay-Loam	0.01	0.5	27000	1750	23
3	Loam	0.5	0.4	21000	2000	37
4	Sandy Loam	10	0.38	16000	1850	37
5	Sand	30	0.41	0	1850	37

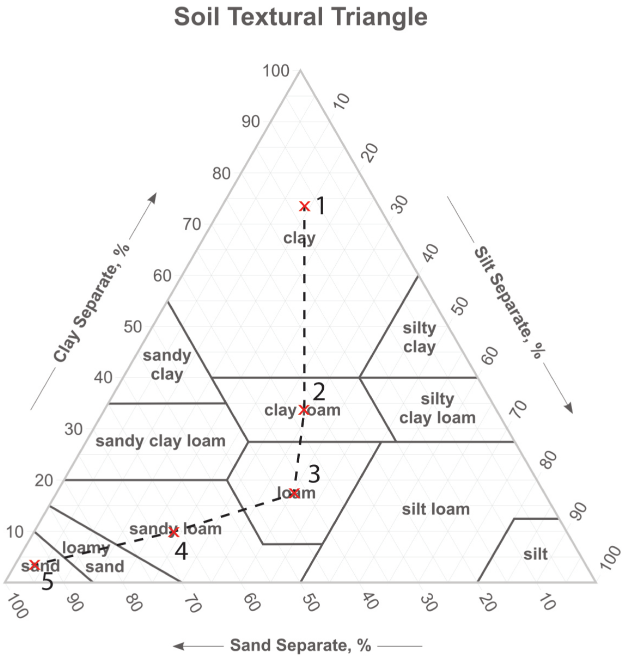

Figure 2. Subsurface types (x) and their interpolation trajectory (dashed line). Soil textural triangle modified from USDA (2017). The numbers correspond with Table 2.

with a large drainage conductance acts as a seepage point that permits outflow only (Hughes et al., 2017). A Newton formulation for unconfined groundwater-flow is used as numerical solution (Niswonger, Panday, & Motomu, 2011).

2.2 Stability model and calculations

The stability calculations in this study were performed as a post-processing with pore pressures obtained from hydraulic heads resulting from the hydrological calculations. The material types (D_{typ}, U_{typ}, L_{typ}) as presented in the previous section, are this time linked to four material parameters important for stability calculations: porosity (P), drained cohesion (C), bulk unit weight (ρ) and effective friction angle (ϕ) (Table 2). Quantitative analysis of stability with probabilistic techniques is done using a limit state function (Z) which is in the form of:

$$Z = |Resistance - Load| \tag{1}$$

To express the relation between resistance and load in a normalized manner, stability is also expressed as a factor of safety (F). The factor of safety is the ratio between resistance and the load, in this case the available shear strength (τ_f) and the developed shear stress (τ_d):

$$F = \frac{\tau_f}{\tau_d} \tag{2}$$

When driving and retaining forces are exactly balanced, it results in a value of $F = 1$ (and $Z = 0$). We further refer to this situation as the limit state of the system. This paper uses steady-state groundwater calculations, which infers that the conductivity of the soils involved is able to dissipate any excess pore-water pressures. Therefor we assume static loading in the sense that non-hydrostatic pore-water pressures are not present at the time of stability calculations, which justifies the use of drained shear strength parameters. The shear strength is thus calculated as a function of the effective stress using the Mohr-Coulomb failure criterion (Terzaghi, 1943).

Though the basic principle and the presence of drained conditions is equal for both basal sliding and soil slip on either side of the dike, their equations differ. For basal sliding, shear strength τ_f is defined along the dike base and τ_d is defined as the force of the water body against the dike. Regarding soil slip on either side of the dike body the Generalized Limit Equilibrium Method (Fredlund & Krahn, 1977; Fredlund, Krahn, & Pufahl, 1981) is used. This method, as a derivation of the Morgenstern-Price method (Morgenstern & Price, 1965), is called a 'best-fit-regression' and solves both moment and force equilibrium on a slip surface for different ratios between the vertical and horizontal inter-slice shear forces. The latter is used to perform a regression on the force and moment equilibrium's, resulting in the final factor of safety (F). In addition, various functions can be used to describe the direction of the inter-slice shear forces, but in our investigation no directional change is considered (Morgenstern & Price, 1965). The factors of safety presented in this paper always represents the factor of safety of the most critical circular slip surface. This surface is found by applying an effective critical slip surface minimization technique adapted from Malkawi, Hassan, and Sarma (2001). To ignore very small slumps not threatening dike macro-stability, a minimum cross-sectional slip surface area of 2 m^2 is imposed. In addition, for soil slip on the outer (river) side of the dike, the stabilizing effect of the high water levels is ignored, which effectively simulates rapid decline of water levels that represent extreme situations (De Waal, 2016).

2.3 Global minimization and sensitivity analysis

The hydro-stability model is used for multiple types of minimization and stability analysis, to obtain the global sensitivity under maximum static groundwater heads and to be able to specify the most sensitive parameters and identify unexpected results. First, the parameter combination leading to the smallest factor of safety, i.e. the globally minimized F, is determined separately for each failure mechanisms within the specified parameter ranges (Table 1). The value of the global minimum, and more important its location in the parameter space, is calculated using a modification of Powell's method (Powell, 1964; Press, Teukolsky, Vetterling, & Flannery, 2007). It performs sequential one-dimensional minimization along each vector of the directions set, which is updated at each iteration of the main minimization loop. Second, taking each mechanism's specific minimum as starting position, a One-at-a-Time (OAT) sensitivity analysis is performed on all parameters. From each of the input parameters 20 samples are taken uniformly out of the likely range (Table 1), while keeping the other parameters at their most unstable condition. Using this parameter set the factor of safety (F) is calculated, which gives a first indication of the parameter-stability relation. The normalized slope quantifies this relation, and is calculated as

$$\bar{S} = (|F_i - F_f|)/(\bar{P}_i - \bar{P}_f) \tag{3}$$

where the subscript i indicates initial values and f indicates sampled values. $\bar{P}$ is the parameter change normalized for its assigned range (Table 1). The steeper the slope $\bar{S}$, the larger the sensitivity of the system to changes in the respective parameter value ($\bar{P}$).

To assess the link between parameters regarding the dike stability, a similar analysis is done from multiple starting situations. In this case, 100 combinations are sampled from all parameters by the latin-hypercube principle retaining multidimensional uniformity (Deutsch & Deutsch, 2012). Given any combination as a starting position, Z (equation 1) is minimized per parameter (OAT), resulting in the parameter value closest to the limit state ($F = 1$) of the system. The normalized slope ($\bar{S}$) is again used as the measure for sensitivity. Parameter combinations that result in a slope deviating from the trend are used to indicate nonlinear behaviour and possibly undesirable dike stability implications.

Finally, a Monte-Carlo (MC) analysis is performed, while again minimizing Z (equation 1). The MC-analysis is based on the six most sensitive parameters (Figure 4), for which eleven values are uniformly chosen within the viable range. This analysis resulted in a very extensive set of parameter combinations closest to the limit state, being a powerful tool to quickly estimate failure probability depending on the uncertainty in some parameters. The data is stored in an extensive database of parameter combinations and their related stability, which can be compared to non-hypothetical situations.

2.4 Importance of hydrology and applications

A non-hypothetical situation is found in a case study of a dike section along the Lek River, The Netherlands. Here this database of MC-analysis results, containing parameter combinations closest to the limit state ($F = 1$), is used for a-priori testing of possibly unreliable dike sections. An actual case is provided by a 3900 meter long dike section near the village of Ameide (51.954594 N, 4.963298 E). Large proportions of this dike have been declared unsafe with respect to the Dutch safety standards (De Waal, 2016) regarding soil slip on both the inner and outer side (Figure 8). To compare the official assessment with the database, the needed data was assembled at an interval of 10 meter along the dike crest. The dike height, crest width and slope were semi-automatically derived from the high resolution AHN3 surface elevation model. The properties of the subsurface, being layer thickness and lithology, are derived from GeoTOP (Stafleu & Dubelaar, 2016). An approximation of the dike lithology is made from publicly available cone penetration tests (BRO) using a simple but effective method proposed by Begemann (1965). Afterwards all combinations from the MC-analysis are selected for which every parameter has a maximum deviation of 25% from the values derived for a given dike section. Based on this selection, the factor of safety belonging to the parameter combination closest to those derived for the dike section is identified, as well as the probability that the safety factor is below $F = 1.5$ (pF), given equally divided probabilities for each parameter combination, as we acknowledge that our simplified method might overestimate the stability. Finally the nearest safety factor and the probability (pF) are compared against the official assessment.

To further analyse the applicability of the steady state results to realistic scenarios, the hydrology and factor of safety were also calculated as a function of time using transient hydrological calculations. The dynamic hydrological model is run for any of the 100 parameter samples created by the latin hypercube sampling (see section 2.2), with a total duration of 20 days and a temporal resolution of one day. The imposed flood starts with the river height at floodplain level which reaches its maximum flood level at the dike crest after one day. At each time step the factor of safety is computed and compared with the steady-state factor of safety for that parameter combination. If the dynamic values differ less than 5% from the static ones, they are assumed similar. This analysis further explores the importance of hydrology in the assessment of dike stability.

3 Results and application

This section will present and discuss the analyses presented in the method section, first focusing on the sensitivity of the dike stability to multiple variations in parameters. Afterwards the results of the Monte-Carlo are presented. Finally, the applicability of the presented results will be discussed.

3.1 Least stable conditions and OAT-sensitivity

The first analysis comprises the determination of the global minimum factor of safety, as well as a OAT-stability analysis starting from that location. The global minimum of the factor of safety is 0.72, 0.52 and 0.54 for basal sliding, soil slip inside and soil slip outside respectively. The absolute lowest factor of safety is found for soil slip on the inside of the dike. In the case of basal sliding, the parameters leading to the minimum factor of safety are all at the edge of the given parameter space (Figure 3). For most parameters this is an indication of a linear system. An illustrative example is the dike slope: The smaller the dike slope, the larger the dike area and its total weight, which increases the resistance against the lateral water pressure and thus increases the stability. However, this is not always the case (section 3.2), as is it in the case of soil slip where this linear behaviour is not observed on all parameters. This is for example the case for the upper layer type (U_{typ}) and the dike height. The results for soil slip on the inner and outer side of the dike are often similar, but striking differences are observed regarding the dike crest width and drainage depth. The dike crest width on the global minimum for inner side soil slip is much larger than where the minimum stability for outer side soil slip is observed. On the other hand, the drainage depth at the global minimum for outer side soil slip is much deeper than for the inside (Figure 3). This likely indicates that the inner side stability is more influenced by the occurrence of drainage, as it is closer to the drainage location (Figure 1).

The OAT-analysis with the location of the global minimum as its starting point is shown in Figure 4. Only those parameters that resulted in any factor of safety change $> 2\%$ are considered. The dike slope (D_s) is clearly one of the main influencing factors, resulting in a factor of safety rise up to 250%. The other main stabilizing factor is the dike type (D_{typ}), which increases the stability as the material gets sandier, mostly owing to the higher ϕ values of sand. For soil slip dike slope and dike material type are in this case the only two parameters that show a clear effect on the dike stability. Many other parameters also have a factor of safety change $> 2\%$ at some value, but their er-

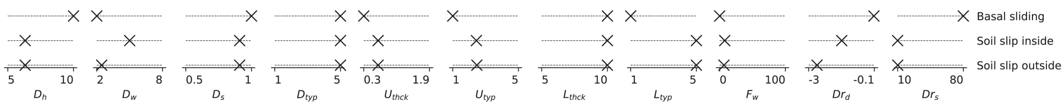

Figure 3. Parameter values resulting in the lowest factor of safety

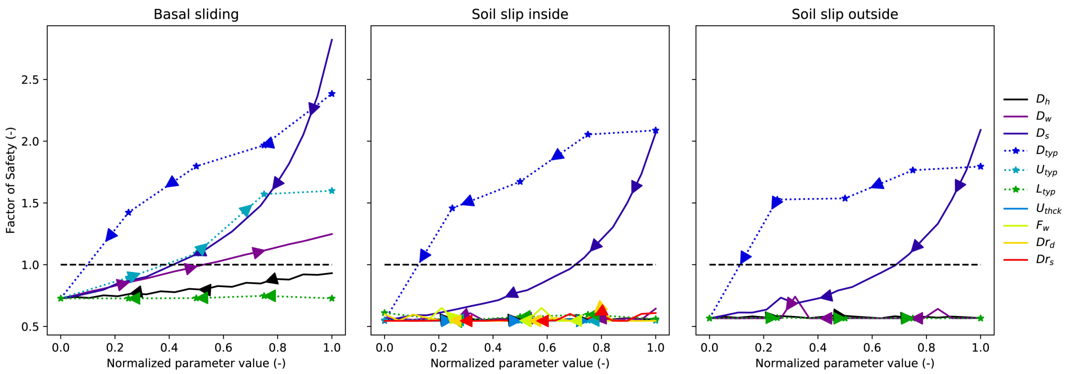

Figure 4. Sensitivity analysis around the least stable value. A normalized parameter value of 0 indicates the global minimum (with the corresponding factor of safety), a value of 1 indicates the other side of the viable parameter range. Arrow direction indicates the direction of non-normalized parameter increase.

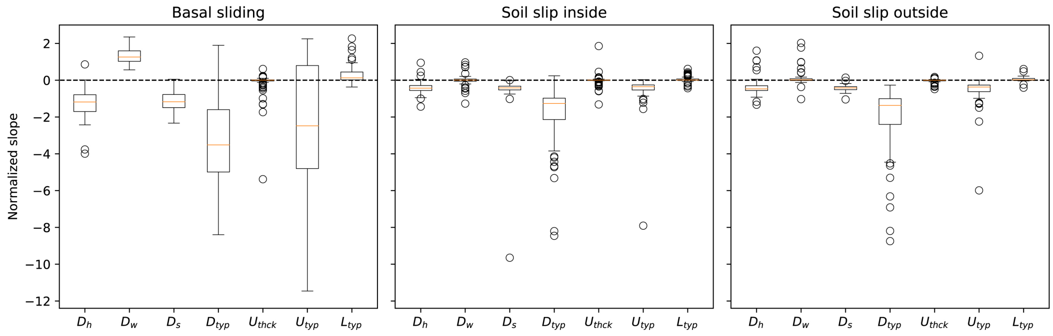

Figure 5. Box-and-whisker plots showing the distribution of safety factors to a change in parameters subject to combinations of parameter values used as the starting point of minimization.

ratic behaviour does not seem to follow a trend. As the influence of these parameters remains small, their nonlinear behaviour only has a minor influence on dike stability. For basal sliding, three more parameters have a large effect, being the upper layer type, dike crest width and dike height. The first two are able to stabilize the dike starting from its global minimum. The parameters with the largest effect were selected for further analysis, being D_h, D_w, D_s, D_{typ}, U_{typ} and L_{typ}. The upper layer thickness (U_{thck}) is also selected as it, despite never showing a clear trend in the previous analysis, is regarded as an important parameter in dike stability analyses regarding soil slip (De Bruijn, de Vries, & 't Hart, 2017).

3.2 Effect of different parameter combinations on sensitivity

When minimizing Z, the starting position of the minimization algorithm has a large effect on the minimized value. When using the parameter values resulting in the minimum stability as the starting point of the sensitivity analysis, only a few parameters are able to stabilize the dike. When using values resulting in a more stable dike as starting position, the chances of reaching $Z = 0$ during minimization are higher. Therefore it is expected that more parameters have an effect if the minimization algorithm advances from different starting locations. This is analysed for the seven selected parameters, of which for 100 parameter combinations generated by latin hypercube sampling, the dike type has the largest influence on the dike stability, indicated by the largest median absolute normalized slope $\bar{S}$ (equation 3). This analysis also corroborates the finding of the previous section that the system appears to be much more sensitive in the case of basal sliding, as in general the normalized slopes have a larger absolute gradient. In general, it can be said that the relative differences in the average parameter sensitivity are in line with the analysis of the global minimized parameter set for each of the failure mechanisms (section 3.1).

The most conspicuous result, however, is that many of the parameters have both a stabilizing as well as a destabilizing effect, as many normalized slopes ($\bar{S}$, Figure 5) can have both positive and negative values. For most parameters, this is limited to few situations, but not for the subsurface types in combination with basal sliding. In the case of basal sliding, the maximum safety factors seem to be reached in case of a similar material in the dike and subsurface layer. Every change away from this equality causes a decrease in dike stability, which nonetheless is faster for sandier material (higher *typ* values). This is caused by the dependence of cohesion (c) and effective friction angle (ϕ) on material type, as stated in Table 2. With the sliding plane at the dike-subsurface interface, basal sliding uses the minimum values of cohesion and friction angle, as they are leading in these situations. So changing either the U_{typ} or D_{typ} to sandier material (higher

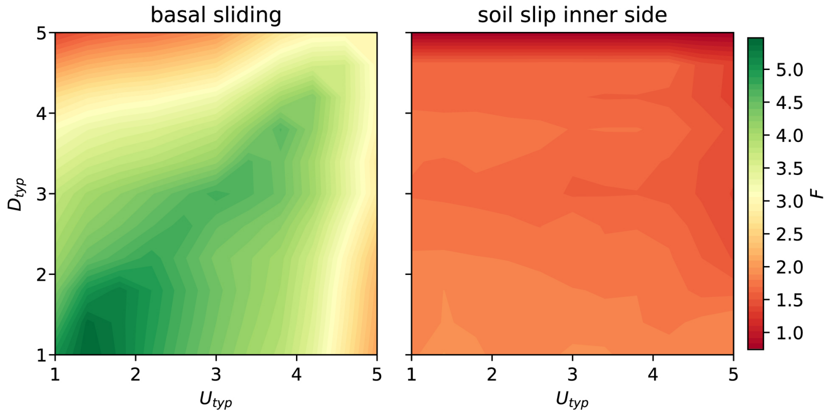

Figure 6. Factor of safety at various combinations of dike type D_{typ} and upper layer type U_{typ}. A clear dependency is visible for basal sliding, where the factor of safety decreases in all directions from a central high, which is not the case for soil slip.

values) from a situation with equal lithologies, causes the minimum value of the dike and upper subsurface layer cohesion to decrease, while the minimum ϕ remains the same. When changing one of the types to more clayey material (smaller values than a situation with equal lithologies), the c remains equal as it is related to the largest subsurface type value, while the ϕ decreases in line with the decreasing subsurface type. For soil slip on any side of the dike this dependency is much less important, as can be seen in Figure 5 by the normalized slope values hardly crossing the dotted zero-line. As shown in Figure 6 the factor of safety decreases with increasing values for U_{typ} as well as D_{typ}, but no maximum is observed at a 1:1 ratio. The larger sensitivity for changes in the dike type are probably caused by the fact that the most critical slip surfaces are mostly located inside the dike, keeping the influence of the upper layer properties limited. Nonetheless, these results underline the importance of a correct subsurface characterization for a reliable dike safety assessment.

3.3 Probability of instability based on Monte Carlo simulations

The Monte Carlo simulations resulted in a database of in total of over 2 million stability calculations, which is available online (van Woerkom, 2020). The most important implications are presented here. Over all calculations, basal siding has a mean factor of safety of 3.57±2.28 and soil slip has a factor of safety of 1.77±0.91 and 2.06±1.13 for the inner and outer side respectively. The fraction of factor of safety values < 1.5 are 0.09, 0.49 and 0.44 respectively. These relatively high fractions are a result of the minimization algorithm, which searches for the F closest to 1. For basal sliding, the mean safety is generally higher, but their larger standard deviation also indicates the larger effect of changes in its parameters on the factor of safety (Figure 7), as also indicated in the previous section. Nonetheless, the soil slip factors of safety are generally closer to critical values, and thus its smaller sensitivities should not be neglected. To further analyze the MC-results, each parameter is equally divided in 10 sections of which the median, 25-75 percentiles and the fraction of $F < 1.5$ (pF) is determined. Looking at the median factor of safety, we again see that the dike slope (D_h) and the dike material type (D_{typ}) have the largest effect. For basal sliding the dike height also has a large influence. For soil slip the factor of safety is mostly determined by the dike parameters, with decreasing safety on increasing dike height, slope and sand fraction of the material. Each parameter's effect becomes especially clear considering pF, which has values up to 0.8 for a sandy dike (normalized dike type = 1), indicating that independent of the value of other

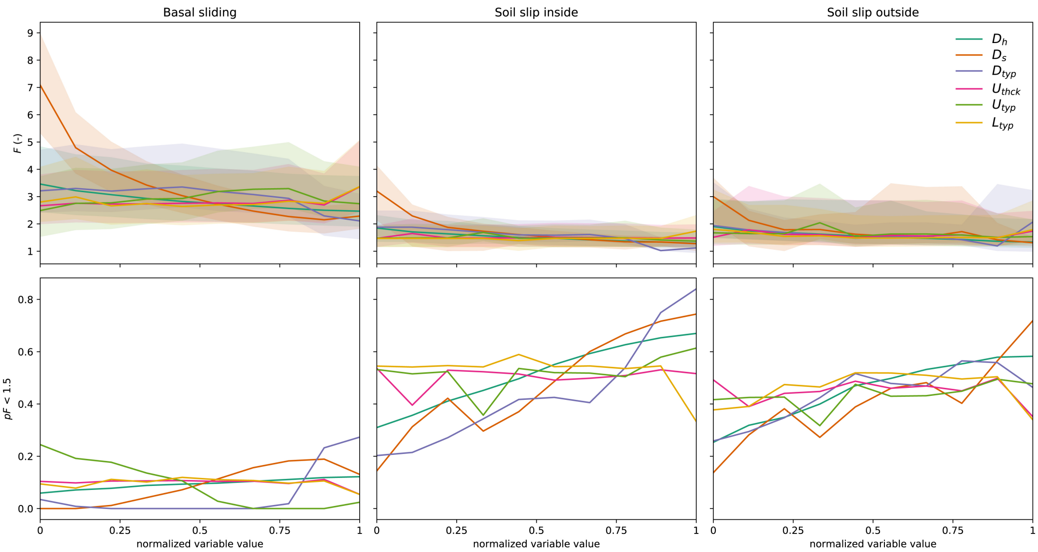

Figure 7. Results of the Monte Carlo simulations for 6 of the most important parameters. The normalized parameter value corresponds with the normalized ranges of the parameters as discussed in Table 1. The shadings indicate the 75 and 25 percentile around the median line.

parameters 80% of all calculated parameter combinations resulted in critical (< 1.5) factors of safety. The counter-intuitive decreasing safety with increasing dike height is caused by the worst-case nature of the assessment, resulting in water levels at the dike crest: A 5 meter high dike with water at its crest results in less strong loading conditions as a 10 meter high dike with water as its crest. The current analysis is done using one constrained parameter, and selecting all MC-results with that parameter value, which implies that only this parameter is known. For an actual dike assessment, increasing knowledge of dike and subsurface parameters can narrow that range constraining more parameters and resulting in a smaller range of possible factors of safety.

3.4 Application of results to case study

Constraining the range of possible parameter values and corresponding factors of safety from the database could be an effective method for a first determination of failure probability for any given dike stretch. This method is applied to a case study area near Ameide, the Netherlands, by comparing the official preliminary dike assessment against the factor of safety in the MC-results, based on parameter values derived for the dike sections from various datasets (see methods 2.4). As both are based on an extreme scenario, we hypothesize that the high sample resolution of the data that will be compared against the database (10 meter) can further inform the official assessment, which is done on a 100 meter resolution. Most importantly, the higher resolution comparison can result in a quick analysis of the most critical sections. On visual inspection, the calculated safety factors already clearly coincide with the official dike assessment (Figure 8), though the variation of the calculated values is much higher, as safety assessments are carried out only per 100 meter section and the factor of safety is calculated every 10 meter. The distinction between the safe and unsafe declared stretches is clear from the database results. On average, the stretches labeled sufficient have a factor of safety of 4.60±0.96 and the insufficient ones of 3.24±1.15. As a result, the probability of unsafe values is mostly zero, indicating that none of the safety factors on comparable cross sections result in a factor of safety below 1.5. On the insufficiently safe sections, our results only predict un-

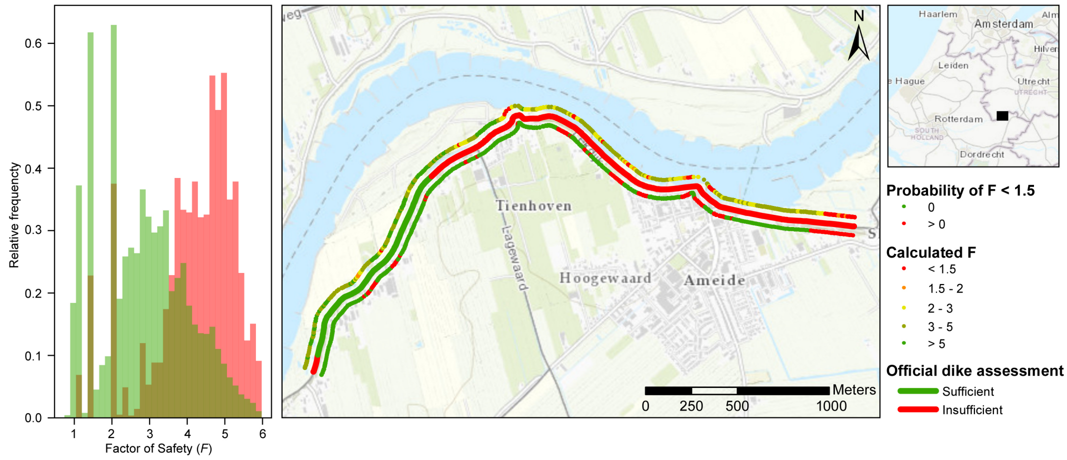

Figure 8. Comparison of determined safety and calculated stability factors for a case study near Ameide, the Netherlands. Left the factor of safety histogram is shown for the sufficient and insufficient sections. The spatial plot shows the official preliminary dike assessment (middle), the nearest calculated factor of safety (above) and the probability of unreliable factors of safety (below).

safe results on 28% of the length, while on the sufficient dike sections, 87% is also seen as sufficient in our results. Still, our high-resolution data disagrees with the official assessment at several locations. In addition to showing high spatial variability in the expected factor of safety, the analysis also clearly shows those sections that according to our calculations are the most critical. These differences might be the result of different data sets that are used as input, but can also be related to some of the parameters (drainage, dynamic river level) that are not included in both analyses. Moreover, it is likely the cause of different definitions of instability (De Waal, 2016). Despite the differences, the high resolution database comparison could help focusing further research in the next stage of dike reinforcement design.

4 Discussion

The hydro-stability model as presented so far is promising, both in providing scientific insights as well as its applicability in safety assessments, but by no means represents the full range of scenarios and variability that can occur. This section analyzes a few more detailed scenarios and explores areas open for improvement.

4.1 Dynamic reality

First, the current steady state hydrological results are compared against a simple dynamic representation. This is done using the sample of 100 parameter combinations (section 3.2), which is also run using a dynamic hydrological model. With a daily timestep, the model is run for 30 days, and each day the factor of safety given the pore pressures at that timestep is compared against the static factor of safety. The results show that after one day, on 17% of the dynamic factors of safety reach similar values. After two days, this percentage increased to 49% and after four days it is 63%. The values of the factor of safety related to lateral push even reach higher values, as finally 95% of the dynamic runs reach similar values. These results show that the presented factors of safety cannot directly be translated to actual situations, but that the relations presented in this paper are strongly indicative of worst-case conditions and therefore a good step in the

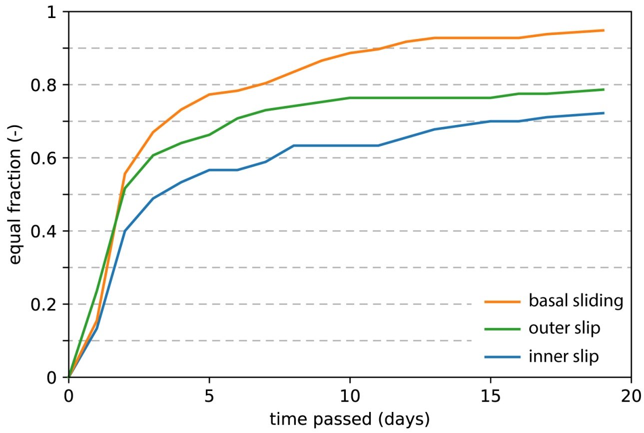

Figure 9. Relation with transient hydrological calculations. The fraction indicates the proportion of the samples that reached similar or lower values than the steady state runs.

direction of understanding dike stability uncertainties. This is indicated by, for example, the flood wave predictions of the Rhine river in the Netherlands (Chbab, den Bieman, & Groeneweg, 2017; Hegnauer, Beersma, van den Boogaard, Buishand, & Passchier, 2014). For a return period of 1250 years the maximum predicted flood wave has a length of approximately 30 days, with expected water levels at values used in this study for up to 11 days. As the predicted height as well as the duration are well within the window in which the steady-state model becomes applicable, many of the results presented in this study can directly be compared against these extreme river stage scenarios. Under dynamic conditions the use of drained loading conditions as a worst-case assessment becomes questionable, but does provide the best comparison with the steady state results. Nonetheless, the hydrological effects of flood wave duration, shape and height would provide a very useful extension of the results presented here.

4.2 Heterogeneity in subsurface and geometry

The subsurface material in this study is assumed homogeneous in each of the layers, as is the layer thickness and surface profile. Due to the long history and continuous improvement of many dikes their interior is presumably very heterogeneous (Olthof et al., 2009). The subsurface characteristics, induced by previous river systems, are also known to have a large spatial variability. These heterogeneous topographic and subsurface characteristics have a large influence on both hydrological conditions (Meehan & Benjasupattananan, 2012; Polanco & Rice, 2014) and stability (Wang, Wang, & Liang, 2018), still ignoring 3D slope effects (Hicks, Nuttall, & Chen, 2014). The simulations show that for all mechanisms, the dike type and upper layer type have a large effect on the dike stability. Despite their importance for dike stability and the valid assumption that they are heterogeneous, these two subsurface parameters are often partly unknown. As a result, mapping their spatial variation, as well as their uncertainty ranges, is of major importance when assessing dike stability (Gong, Tang, Wang, Wang, & Juang, 2019). Incorporating large scale subsurface heterogeneity (in 3D) is another important step in actively incorporating groundwater calculations in dike stability calculations. A secondary aspect that is often important in 3D scenarios of dike reliability is the remaining strength of the dike, as soil slip does not necessarily induce breaching. Al those factors might influence the results presented in this paper, and probably result in even lower factors of stability. However, we are confident that the presented results do provide an analysis of the complete hydro-stability system, incorporating the most important factors at first order. Furthermore, the database constructed for and reviewed in this paper is very suitable for identifying those regions where factors of safety might reach critical values when subsurface uncertainty is included. By downsizing the region, more direct, accurate and cost effective investigations can be made in the process previous to the actual enforcement (Delta Commissie, 2008).

5 Conclusion

In this study an extensive sensitivity analysis is carried out for dike stability using steady-state calculated groundwater heads and resulting pore pressures, which are indicative of worst case scenarios. The results show that each of the three studied failure mechanisms, being basal sliding and soil slip on the inner and outer side, can possibly result in dike failure. Nonetheless, dike stability by basal sliding is generally more sensitive to changes in the parameters. The shallow subsurface material is important for basal sliding, in addition to the dike slope and material which are also the most important for all three mechanisms. The direction of change is mostly uniform for a change in parameter value, but the magnitude is highly variable, also when changing a single parameter. An exception on this rule is the relation between dike material and confining layer material, which may either decrease and increase the stability based on the ratio between the two. The results of the Monte-Carlo simulation provides a exhaustive method of quantifying possible critical combinations. The fraction of combinations that possibly lead to failure ($F < 1.5$) is much higher for soil slip (0.47, 0.52) than for basal sliding (0.09). Furthermore, full probabilistic research is needed for increased precision, in addition to the inclusion of currently unconsidered parameters as small scale subsurface heterogeneity, remaining strength and dynamic loading conditions. Nonetheless, applying our results to a case study dike with a simple and effective method results in high-resolution data on dike stability that corroborates reasonably well with official inspection results. Together with the sensitivity of the system to changes in individual parameters, this result provides useful insights in the process and effect of dike and subsurface parameters on groundwater-related dike stability.

Acknowledgments

This project was supported by funding from the Netherlands Organisation for Scientific Research (NWO-TTW) within the All-risk project (grant no. P15-21). TvW, MB and HM developed the research goal. TvW and RvB performed the primary data analysis and model development. HM and MB helped with result interpretation. The authors declare no competing interests. The support of Edwin Sutanudjaja and Lukas van de Wiel enabling the computational power needed for the Monte Carlo simulations is also greatly appreciated. The results from this analysis as presented are online available (doi:10.5281/zenodo.3630154, van Woerkom (2020)).

References

Begemann, H. (1965). The Friction Jacket Cone as an Aid in Determining the Soil Profile. *Proceedings of the 6th International Conference on Soil Mechanics and Foundation Engineering, ICSMFE.*, 8–15.

Berendsen, H. J. (1982). De genese van het landschap in het zuiden van de provincie Utrecht. *Utrechtse Geografische Studies*, *25*, 259.

Chbab, H., den Bieman, J., & Groeneweg, J. (2017). *Hydraulische Belastingen Rijntakken en Maas* (Tech. Rep.). Deltares.

De Bruijn, H., de Vries, G., & 't Hart, R. (2017). *Voorschrift Toetsen op Veiligheid, Technisch Deel* (Tech. Rep. No. Wti).

De Waal, J. P. (2016). *Basisrapport WBI 2017* (Tech. Rep.).

Delta Commissie. (2008). *Samen werken met water* (Tech. Rep.). Retrieved from `http://www.deltacommissie.com/doc/2008-09-03AdviesDeltacommissie.pdf`

Deutsch, J. L., & Deutsch, C. V. (2012, mar). Latin hypercube sampling with multidimensional uniformity. *Journal of Statistical Planning and Inference*, *142*(3), 763–772. Retrieved from `https://www.sciencedirect.com/science/article/pii/S0378375811003776` doi: 10.1016/j.jspi.2011.09.016

Eijgenraam, C., Kind, J., Bak, C., Brekelmans, R., Den Hertog, D., Duits, M., ... Kuijken, W. (2014, jan). Economically efficient standards to protect the netherlands against flooding. *Interfaces*, *44*(1), 7–21. doi: 10.1287/inte.2013.0721

Förster, U., van den Ham, G., Calle, E., & Kruse, G. (2012). *Zandmeevoerende Wellen* (Tech. Rep.). Ministerie van Infrastructuur & Milieu. doi: 1202123-003

Fredlund, D. G., & Krahn, J. (1977, aug). Comparison of slope stability methods of analysis. *Canadian Geotechnical Journal*, *14*(3), 429–439. Retrieved from `http://www.nrcresearchpress.com/doi/10.1139/t77-045` doi: 10.1139/t77-045

Fredlund, D. G., Krahn, J., & Pufahl, D. E. (1981). The Relationship between Limit Equilibrium Slope Stability Methods. In *Proceedings of the international conference on soil mechanics and foundation engineering* (pp. 409–416). Stockholm. Retrieved from `https://www.soilvision.com/subdomains/unsaturatedsoil.com/Docs/ResearchPapers/1981/ConferencePapers/Therelationshipbetweenlimitequilibriumslopestabilitymethods.pdf`

Gong, W., Tang, H., Wang, H., Wang, X., & Juang, C. H. (2019, sep). Probabilistic analysis and design of stabilizing piles in slope considering stratigraphic uncertainty. *Engineering Geology*, *259*. doi: 10.1016/j.enggeo.2019.105162

Hegnauer, M., Beersma, J., van den Boogaard, H., Buishand, T., & Passchier, R. (2014). *Generator of Rainfall and Discharge Extremes (GRADE) for the Rhine and Meuse basins. Final report of GRADE 2.0* (Tech. Rep.). Retrieved from `http://projects.knmi.nl/publications/fulltexts/1209424004zws0018rgenerator{\_}of{\_}rainfall{\_}and{\_}discharge{\_}extremes{\_}grade{\_}for{\_}the{\_}rhine{\_}and{\_}meuse{\_}basins{\_}definitief.pdf`

Hicks, M. A., Nuttall, J. D., & Chen, J. (2014). Influence of heterogeneity on 3D slope reliability and failure consequence. *Computers and Geotechnics*, *61*, 198–208. doi: 10.1016/j.compgeo.2014.05.004

Hughes, J., Langevin, C., & Banta, E. (2017). *Documentation for the MODFLOW 6 Framework* (Tech. Rep.). Retrieved from `https://pubs.er.usgs.gov/publication/tm6A57` doi: 10.1111/jcpe.12251[doi]

ICOLD, C. (2018). Twenty-Sixth Congress on Large Dams / Vingt-Sixieme Congres des Grands Barrages: : 4th - 6th July 2018, Vienna, Austria. In (1st ed., p. 4571). CRC Press.

IPCC, W. I. (2014). *Summary for Policymakers* (Tech. Rep.). Retrieved from https://www.ipcc.ch/pdf/assessment-report/ar5/wg3/ipcc{_}wg3{_}ar5{_}summary-for-policymakers.pdf doi: 10.1017/CBO9781107415324

Langevin, C., Hughes, J., Banta, E., Provost, A., Niswonger, R., Panday, & Sorab. (2018). *MODFLOW 6 Modular Hydrologic Model version 6.0.3.* U.S.G.S. Retrieved from https://www.usgs.gov/software/modflow-6-usgs-modular-hydrologic-model{\#}mf6pubs doi: https://doi.org/10.5066/F76Q1VQV

Lanzafame, R., Teng, H., & Sitar, N. (2017). Stochastic Analysis of Levee Stability Subject to Variable Seepage Conditions. In *Geotechnical special publication* (pp. 554–563). doi: 10.1061/9780784480700.053

Malkawi, A. H., Hassan, W. F., & Sarma, S. K. (2001, oct). An efficient search method for finding the critical circular slip surface using the Monte Carlo technique. *Canadian Geotechnical Journal*, *38*(5), 1081–1089. Retrieved from http://www.nrcresearchpress.com/doi/10.1139/t01-026 doi: 10.1139/t01-026

Mateo-Lázaro, J., Sánchez-Navarro, J. Á., García-Gil, A., Edo-Romero, V., & Castillo-Mateo, J. (2016). *Modelling and layout of drainage-levee devices in river sections* (Vol. 214; Tech. Rep.). Retrieved from http://dx.doi.org/10.1016/j.enggeo.2016.09.011 doi: 10.1016/j.enggeo.2016.09.011

Meehan, C. L., & Benjasupattananan, S. (2012). An analytical approach for levee underseepage analysis. *Journal of Hydrology*, *470-471*, 201–211. Retrieved from http://dx.doi.org/10.1016/j.jhydrol.2012.08.050 doi: 10.1016/j.jhydrol.2012.08.050

Middelkoop, H., Daamen, K., Gellens, D., Grabs, W., Kwadijk, J. C. J., Lang, H., … Wilke, K. (2001). Impact of climate change on hydrological regimes and water resources management in the Rhine basin. *Climatic Change*, *49*(1-2), 105–128. Retrieved from http://link.springer.com/10.1023/A:1010784727448 doi: 10.1023/A:1010784727448

Morgenstern, N. R., & Price, V. E. (1965, mar). The Analysis of the Stability of General Slip Surfaces. *Géotechnique*, *15*(1), 79–93. Retrieved from http://www.icevirtuallibrary.com/doi/10.1680/geot.1965.15.1.79 doi: 10.1680/geot.1965.15.1.79

Niswonger, R. G., Panday, S., & Motomu, I. (2011). *MODFLOW-NWT , A Newton Formulation for MODFLOW-2005* (Tech. Rep.). Retrieved from https://pubs.usgs.gov/tm/tm6a37/pdf/tm6a37.pdf

Olthof, B., van Boheemen, Y., Danner, H., Hooiveld, M., & de Vries, D. (2009). *Beeldkwaliteitsplan Westfriese Omringdijk* (Tech. Rep.). Provincie Noord-Holland. Retrieved from www.westfrieseomringdijk.nl

Peñuela, W. F. M. (2013). *River dyke failure modeling under transient water conditions* (Doctoral dissertation). doi: 10.3929/ETHZ-A-010088952

Polanco, L., & Rice, J. (2014). A Reliability-Based Evaluation of the Effects of Geometry on Levee Underseepage Potential. *Geotechnical and Geological Engineering*, *32*(4), 807–820. Retrieved from https://link.springer.com/content/pdf/10.1007{\%}2Fs10706-014-9759-2.pdf doi: 10.1007/s10706-014-9759-2

Powell, M. J. D. (1964, feb). An efficient method for finding the minimum of a function of several variables without calculating derivatives. *The Computer Journal*, *7*(2), 155–162. Retrieved from https://academic.oup.com/comjnl/article-lookup/doi/10.1093/comjnl/7.2.155 doi: 10.1093/comjnl/7.2.155

Press, W. H., Teukolsky, S. A., Vetterling, W. T., & Flannery, B. P. (2007). *Numerical recipes : the art of scientific computing.* Cambridge University Press.

Richards, K. S., & Reddy, K. R. (2007). Critical appraisal of piping phenomena in earth dams. *Bulletin of Engineering Geology and the Environment*, *66*(4), 381–402. Retrieved from http://www.npdp.stanford.edu/index.html doi: 10

.1007/s10064-007-0095-0

Stafleu, J., & Dubelaar, C. W. (2016). *Product specification Subsurface model GeoTOP* (Tech. Rep.). Retrieved from `www.tno.nl`

Stanisz, J., Borecka, A., Pilecki, Z., & Kaczmarczyk, R. (2017). Numerical simulation of pore pressure changes in levee under flood conditions. In *E3s web of conferences* (Vol. 24). Retrieved from `https://www.e3s-conferences.org/articles/e3sconf/pdf/2017/12/e3sconf{\_}ag2017{\_}03002.pdf` doi: 10.1051/e3sconf/20172403002

Stark, T. D., Choi, H., & Lee, C. (2009). Case study of undrained strength stability analysis for dredged material placement areas. *Journal of Waterway, Port, Coastal and Ocean Engineering*, *135*(3), 91–99. doi: 10.1061/(ASCE)0733-950X(2009)135:3(91)

Terzaghi, K. (1943). *Theoretical Soil Mechanics.* Hoboken, NJ, USA: John Wiley & Sons, Inc. Retrieved from `http://doi.wiley.com/10.1002/9780470172766` doi: 10.1002/9780470172766

Tourment, R. (2018). *European and US levees and flood devences; Characteristics, Risks and Governance* (Tech. Rep.). EUCOLD Working Group on Levees and Flood Defences. Retrieved from `www.barrages-cfbr.eu`

USDA. (2017). *Soil Survey Manual* (3rd ed.; S. S. D. Staff, Ed.).

Vahedifard, F., Sehat, S., & Aanstoos, J. V. (2017). Effects of rainfall, geomorphological and geometrical variables on vulnerability of the lower Mississippi River levee system to slump slides. *Georisk*, *11*(3), 257–271. Retrieved from `http://www.tandfonline.com/action/journalInformation?journalCode=ngrk20` doi: 10.1080/17499518.2017.1293272

van Woerkom, T. A. A. (2020). *Monte-Carlo simulation of dike stability based on a coupled steady-state hydro-stability model.* Zenodo. doi: 10.5281/zenodo.3630154

Wang, X., Wang, H., & Liang, R. Y. (2018, may). A method for slope stability analysis considering subsurface stratigraphic uncertainty. *Landslides*, *15*(5), 925–936. doi: 10.1007/s10346-017-0925-5